

Low-temperature specific-heat anomalies associated with the boson peak in CuZr-based bulk metallic glasses

Yong Li, H. Y. Bai,* and W. H. Wang

Institute of Physics, Chinese Academy of Sciences, Beijing 100080, China

K. Samwer

I. Physikalisches Institut, Universität Göttingen, Göttingen D-37077, Germany

(Received 16 June 2006; published 4 August 2006)

We report the pronounced low-temperature specific-heat C_p anomalies associated with the boson peak in the new CuZr-based bulk metallic glasses. The origin of the C_p anomalies in the atomic glasses is interpreted with the harmonic localized mode based on the dense-packed atomic clusters structural model of metallic glass. The results might have important implications for understanding the origin of the boson peak and the structural features of metallic glasses.

DOI: 10.1103/PhysRevB.74.052201

PACS number(s): 61.43.Dq, 63.50.+x, 81.05.Kf

One of the most intriguing universal features of glasses, observable in Raman or inelastic neutron scattering, is the so-called boson peak (BP), which is defined as excess with respect to the Debye contribution in the low-frequency vibrational density of state (VDOS).^{1,2} At low T , accordingly, the specific heat C_p of glasses often presents a distinct excess in C_p/T^3 compared to the Debye theory above 1 K, which is related to the BP contribution. Many competing models as to the origin of the BP have been proposed.³⁻⁶ Interest in this issue is further stimulated by the finding that the amplitude of BP is even correlated with the liquid fragility m [defined as the change of viscosity η with T approaching glass transition T_g (Ref. 7)] in nonmetallic glasses.⁶ However, the origin of BP is still a debated issue and is commonly considered as one of the great mysteries of glass physics. It is also unclear how general such an anomaly might be in various glasses and how it relates to glassy features. Furthermore, previous studies on BP mainly concentrated on network or polymeric glasses. The nature of BP is difficult to understand well only by investigating the molecular glasses because the intramolecular, reorientational, and translational motions of molecules in these glasses all may contribute to BP. Metallic glass with a simple atomic glassy structure (without reorientation and intramolecular processes) could provide clearer evidence for the underlying physics of BP. However, the metallic glasses with a close-packed Bernal structure are rarely reported yet among the materials that develop the BP.⁸

Recently, we developed a binary CuZr bulk metallic glass (BMG). Based on the BMG, a series of novel BMGs with significant differences in glass-forming ability (GFA), elastic properties, and configurational features was obtained by minor additions. Particularly, the BMGs cover a substantial part of the Angell diagram in terms of fragility⁷ and show specific-heat anomaly.⁸ The availability of such glasses makes it possible to study the low- T C_p anomaly associated with the generation of low-frequency modes. We report the pronounced low- T C_p anomalies in the BMGs. We find that the C_p anomalies can be attributed to a harmonic localized Einstein mode in the simple atomic glasses with a dense-packed solute-atom-centered cluster structure.

Three representative BMGs, $\text{Cu}_{50}\text{Zr}_{50}$, $(\text{Cu}_{50}\text{Zr}_{50})_{96}\text{Al}_4$,

and $(\text{Cu}_{50}\text{Zr}_{50})_{90}\text{Al}_7\text{Gd}_3$, with markedly different properties are chosen as model glasses to study C_p at low temperatures. The preparation of the BMGs can be referred to in Ref. 10. For the C_p measurements, the square-shaped plates with a size of $3 \times 2 \times 1 \text{ mm}^3$ were used. The C_p was measured by the Physical Property Measurement System using PPMS 6000 with an accuracy of about 2%. The fragility m of the BMGs was determined thermodynamically, which was confirmed by previous studies equally well as complementary viscosity measurements.¹¹ Table I lists the parameters of GFA, fragility, elastic properties, and microstructural features of the BMGs. The $\text{Cu}_{50}\text{Zr}_{50}$ is one of the most fragile BMGs known; the $(\text{Cu}_{50}\text{Zr}_{50})_{90}\text{Al}_7\text{Gd}_3$ is one of the strongest BMGs known; and the $(\text{Cu}_{50}\text{Zr}_{50})_{96}\text{Al}_4$ BMG possesses an intermediate degree of fragility.¹¹

The inset of Fig. 1 presents T -dependent C_p of the BMGs

TABLE I. The fragility m , critical sample thickness d_c , volume per mole V_m , and Poisson ratio ν for the CuZr-based BMGs. The marked increase of d_c indicates the significant increase of the GFA of the alloys by minor additions (Ref. 9). The fitting coefficients (γ and β) from the least-square linear fit of $C_p/T = \gamma + \beta T^2$ below the temperature 8 K, the BP amplitude $[(C_p - \gamma T)/T^3]_{\text{max}}$ and position T_{max} , the θ_D (β_D), and the θ_E from the fitting results of $C_p = \gamma T + C_D + n_E C_E$ in the whole measured temperature region are also listed, where $C_D = n_D 3R(T/\theta_D)^3 \int_0^{\theta_D/T} \xi^4 e^\xi / (e^\xi - 1)^2 d\xi$.

Parameter	$\text{Cu}_{50}\text{Zr}_{50}$	$(\text{Cu}_{50}\text{Zr}_{50})_{96}\text{Al}_4$	$(\text{Cu}_{50}\text{Zr}_{50})_{90}\text{Al}_7\text{Gd}_3$
d_c (mm)	2	5	10
m	62	40	30
V_m (cm^3)	10.4	10.5	10.7
ν	0.359	0.369	0.373
γ (mJ/mol K ²)	4.3	3.7	4.9
β (mJ/mol K ⁴)	0.12	0.18	0.20
T_{max} (K)	16.4	10.1	7.8
$[(C_p - \gamma T)/T^3]_{\text{max}}$	0.123	0.176	0.204
θ_D (K)	279	275	268
β_D (mJ/mol K ⁴)	0.090	0.094	0.101
θ_E (K)	83	50	36

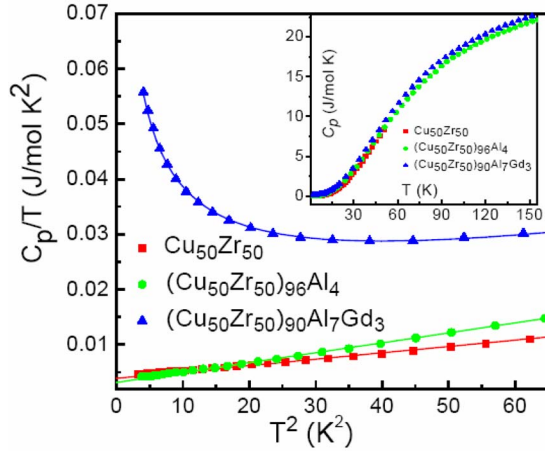


FIG. 1. (Color online) The C_p/T vs T^2 plots for $\text{Cu}_{50}\text{Zr}_{50}$, $(\text{Cu}_{50}\text{Zr}_{50})_{96}\text{Al}_4$, and $(\text{Cu}_{50}\text{Zr}_{50})_{90}\text{Al}_7\text{Gd}_3$ BMGs. Solid lines are the fitting results from 2 to 8 K. The inset is the T -dependent C_p of these BMGs in large T range.

down to 2 K. The C_p of CuZr BMG is in agreement with the data of Ref. 11 where the rapidly quenched ribbon was used. To analyze the data, one needs to determine the electronic contribution to C_p correctly. The C_p below 8 K is displayed in a C_p/T vs T^2 plot in Fig. 1. A least-square linear fit of $C_p/T = \gamma + \beta T^2$ is used to determine the electronic coefficient γ by extrapolating the fitting curve to 0 K. (The superconducting temperature of CuZr glass is < 2 K.¹²) For $(\text{Cu}_{50}\text{Zr}_{50})_{90}\text{Al}_7\text{Gd}_3$ BMG below 8 K, there exists a constant contribution to C_p , which comes from Gd-addition-induced magnetic clusters in the BMG. Its C_p is described by

$$C_p = \gamma T + \beta T^3 + A, \quad (1)$$

with the constant contribution $A = 100.08$ m J/mol K. All the fitting coefficients are compiled in Table I.

Figure 2 shows the $(C_p - \gamma T)/T^3$ of the BMGs without the mask of the electronic and/or magnetic contributions. The results clearly exceed the Debye model and show an anomaly. The fragile CuZr glass shows a hardly pronounced

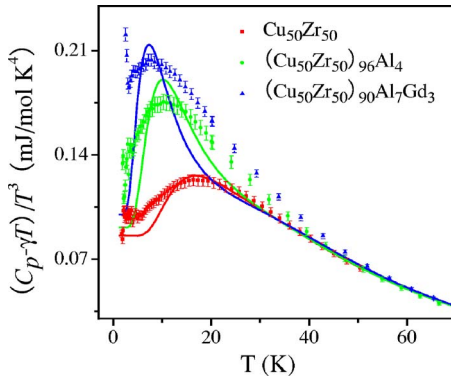


FIG. 2. (Color online) The $(C_p - \gamma T)/T^3$ vs T plots of $\text{Cu}_{50}\text{Zr}_{50}$, $(\text{Cu}_{50}\text{Zr}_{50})_{96}\text{Al}_4$, and $(\text{Cu}_{50}\text{Zr}_{50})_{90}\text{Al}_7\text{Gd}_3$ BMGs after subtracting the electronic contribution and/or the magnetic contribution. The adequate fits of the C_p of the three BMGs with the Einstein mode are also shown.

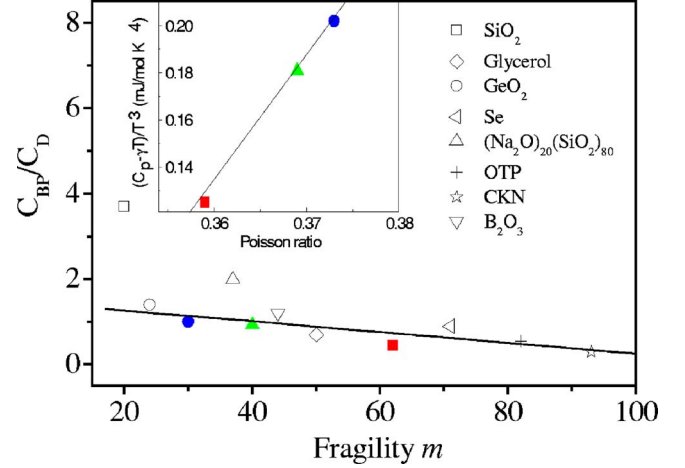


FIG. 3. (Color online) The ratio of the BP contribution to the Debye contribution around the maximum (at 7–18 K) vs the fragility m of $\text{Cu}_{50}\text{Zr}_{50}$ (■), $(\text{Cu}_{50}\text{Zr}_{50})_{96}\text{Al}_4$ (▲), and $(\text{Cu}_{50}\text{Zr}_{50})_{90}\text{Al}_7\text{Gd}_3$ (●) BMGs and other nonmetallic glasses. The data of the nonmetallic glasses are from Ref. 6 and references therein. The θ_D of the BMGs come from the fitting results of Fig. 4. The inset is the $[(C_p - \gamma T)/T^3]_{\max}$ vs Poisson ratio ν of $\text{Cu}_{50}\text{Zr}_{50}$ (■), $(\text{Cu}_{50}\text{Zr}_{50})_{96}\text{Al}_4$ (▲), and $(\text{Cu}_{50}\text{Zr}_{50})_{90}\text{Al}_7\text{Gd}_3$ (●) BMGs.

bump, which is general for other fragile glasses.⁶ The bump becomes more pronounced, and the T_{\max} corresponding to the maximum excess C_p shifts to lower T for the stronger BMGs. As in many nonmetallic glasses, it is reasonable to believe that the bumps arise from low-frequency vibrations and correspond to the BP.^{2–4}

The value $[(C_p - \gamma T)/T^3]_{\max}$ at the maximum for the BMGs increases with the decreasing m , and the excess C_p becomes much stronger in the strong BMGs. The values $(C_p/T^3)_{\max}$ of the oxide and organic glasses are 10–20 times larger than those of BMGs because of the large Debye contribution to C_p of the nonmetallic glasses.^{6,13–15} The C_{BP} is obtained from subtracting the Debye contribution, γT , and/or the magnetic contribution from the measured C_p ,

$$C_{BP}/C_D = (C_p - C_D - \gamma T - A)/C_D. \quad (2)$$

After scaling by C_D , the different Debye contributions which are usually the major ones to C_p are eliminated; the C_{BP}/C_D values of the BMGs, oxide glasses, and organic glasses obey a correlation between the BP and m only with the exception of SiO_2 (Ref. 16) (see Fig. 3). The inset of Fig. 3 and Table I also show that the BP strength correlates with Poisson ratio ν and GFA.⁶

The C_p of solids in wide T range normally can be explained by the Debye model. However, the C_p in large T range of these BMGs cannot be well fitted only by the Debye and the electron contributions. We found that an additional Einstein mode is required to fit the C_p adequately. This is illustrated in Fig. 4 for CuZr BMG. The solid line in Fig. 4 represents a fit

$$C_p = \gamma T + C_D + n_E C_E, \quad (3)$$

where C_D represents the Debye term with $\theta_D = 279$ K; C_E is the Einstein term

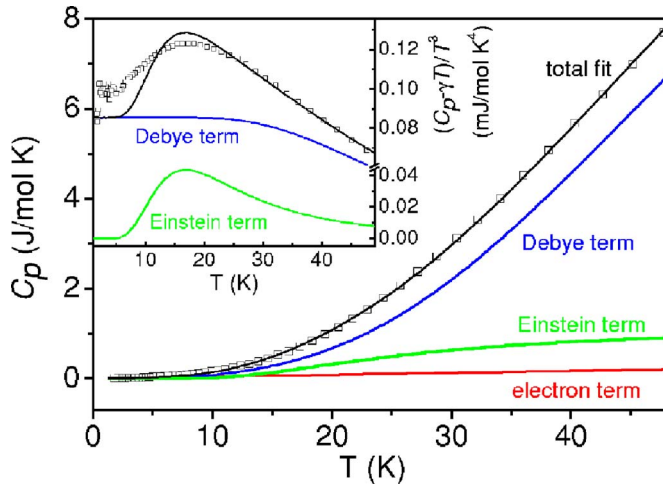


FIG. 4. (Color online) The fitting results (solid lines) including the contributions of the Debye mode and one Einstein mode of the C_p of $\text{Cu}_{50}\text{Zr}_{50}$ BMG between 2 and 50 K. The inset presents the data as $(C_p - \gamma T)/T^3 \sim T$.

$$C_E = R \left(\frac{\theta_E}{T} \right)^2 \frac{e^{\theta_E/T}}{(e^{\theta_E/T} - 1)^2}, \quad (4)$$

with an Einstein temperature $\theta_E = 83$ K, and the Einstein oscillator strength per mole $n_E = 0.14$. The adequate fits with the Einstein mode of the BMGs are shown in Fig. 2. We also find that the existence of the Einstein oscillators is ubiquitous for the variety of BMGs available.

The VDOS can be derived from the C_p .¹⁷ The derived total VDOS of the CuZr-based BMGs in the units of oscillators per mole is shown in Fig. 5. Clearly the Einstein mode induces a peak below 10 meV. Because there are no existing experimental VDOS data for the CuZr-based BMGs, we measured the C_p of a $\text{Zr}_{46.75}\text{Ti}_{8.25}\text{Cu}_{7.5}\text{Ni}_{10}\text{Be}_{27.5}$ BMG

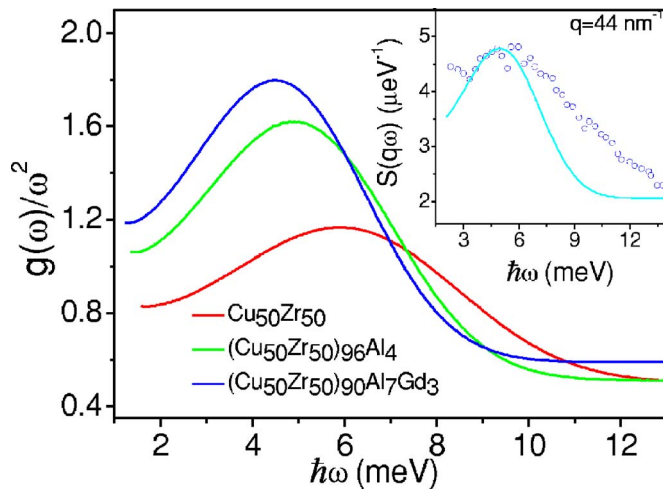


FIG. 5. (Color online) The derived total VDOS of the BMGs. The inset shows derived VDOS of vit4 from the C_p and neutron inelastic scattering (Ref. 17). Vit4 has an Einstein mode with $\theta_E = 74$ K. The agreement rather supports a picture in which the boson peak in the metallic glasses is ascribed to the localized vibrations modes.

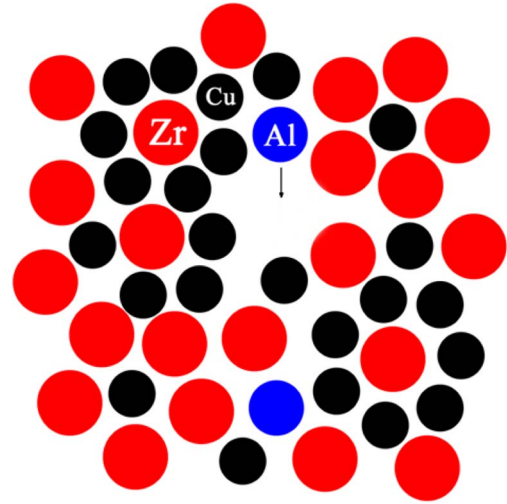


FIG. 6. (Color online) A 2D representation of a dense-packed solute-atom-centered cluster structure (Ref. 20). The black and red spheres denote the solvent atoms, and the blue spheres denote the solute atoms with different diameters that can play the role of the loose atoms and induce the independent localized harmonic mode.

(vit4). The experimental VDOS from neutron inelastic scattering¹⁸ and the derived VDOS from C_p of vit4 are shown in the inset of Fig. 5. In vit4, the peak at 4.9 meV induced by the Einstein oscillator in the derived VDOS from C_p has almost the same energy and similar shape as the BP (about 5 meV) determined by neutron scattering.¹⁸ The observations and the agreement rather support a picture in which the BP in the metallic glasses is ascribed to the localized vibrations modes.

It is striking that the Einstein model appears to work well for the BP in metallic glasses while it does not work in other glasses. The presence of an Einstein oscillator suggests the existence of the vibrations of loose atoms in an independent localized harmonic mode in the glasses. In crystalline materials, the vibrations of the loose “rattler” atoms in the oversized cage structure or large voids are thought to result in the localized modes.¹⁷ The crystalline-like behavior in the BMGs may result from the unique structural features of the BMGs. The experimental and simulation evidence show that the nearest-neighbor atomic structure in BMGs displays order alike that in crystalline materials.^{19,21} The dense cluster-packing model is schematically illustrated in Fig. 6.²¹ The spherulike clusters (~ 0.7 – 1.0 nm) are efficiently packed to fill the space, and defects can also exist within the dense-packed clusters. The cluster-formed glass also includes solutes that occupy the interstices in the cluster assemblages. This model accurately provides richness to the structural description of BMGs and a remarkable ability to predict BMG compositions for various alloys. This model is helpful for understanding the BP in BMGs. Some of the solute atoms which are independent of others can play the role of the loose atoms, and the vibrations of rattlinglike loose solute atoms are thought regarded to induce the independent localized harmonic mode similar to that found in compounds.^{17,22}

In the theoretical view, the mode-coupling theory (MCT) (Ref. 23) is one of the successful theories that can predict a

qualitative change in microscopic dynamics and glass transition in supercooled liquids. MCT predicts a faster β relaxation that can be visualized as a rattling of the atoms in the transient cages.²³ Recent molecular simulations of a NiZr melt strongly suggest that β relaxation as a precursor of structural relaxation occurs also in metallic glasses.²⁴ Meyer *et al.*¹⁸ observed such a fast β relaxation in BMG-forming liquid, in full accord with MCT, and some metallic glasses showed stronger harmonic behavior than most crystalline solids. The BMGs, obtained by quick quenching from the liquids, to some extent can inherit liquid structure and contain a large number of cages and free volumes. The atoms sitting in the oversized cage or in sufficiently large free volumes are loose and can vibrate in independent harmonic modes. The assumption is confirmed to some extent by Angell,²⁵ who found a much stronger BP in hyperquenched glasses.

A truly localized mode appears as a δ function in the VDOS. However, most of the solute atoms located at different cluster interstices are easy to hybridize with other acoustic phonons. Therefore, the mode's contribution to VDOS has a Gaussian distribution deviating from the Debye mode.¹⁷ At high T (>10 meV), the hybridization with other

modes is stronger, and the peak is considerably broader, which cannot be separated from the measurement. At low enough T , some of the modes are strongly hybridized with extended phonons, and the "local" character is eliminated, which may be reduced to a TLS. In fact, the BP at ~ 5.9 meV for $\text{Cu}_{50}\text{Zr}_{50}$ is broader than that of $(\text{Cu}_{50}\text{Zr}_{50})_{96}\text{Al}_4$ (~ 4.9 meV) and $(\text{Cu}_{50}\text{Zr}_{50})_{90}\text{Al}_7\text{Gd}_3$ (~ 4.5 meV) (see Figs. 2 and 5). The θ_E decreases with the increasing addition, indicating the strengthening of the Einstein mode with the changing structure. In the alloys, the minor addition of atoms (Al and Gd) with markedly different atomic sizes induces an increase of the amount of the solute atoms and vacancies, and then changes the localized vibrations. This causes the change of the position, the intensity, and the broadness of the BP. Ultrasonic and density measurements (Table I) confirm that the additions do induce marked changes in moduli and molar volume, indicating obvious structural change.

We thank P. O. Pohl for a critical reading of the manuscript. The support of the NSFC (Contracts No. 50225101 and No. 50321101), DFG, and Leibniz program are appreciated.

*Electronic address: hybai@aphy.iphy.ac.cn

¹U. Buchenau, N. Nucker, and A. J. Dianoux, *Phys. Rev. Lett.* **53**, 2316 (1984).

²F. Sette, M. H. Krisch, C. Masciovecchio, G. Ruocco, and G. Monaco, *Science* **280**, 1550 (1998).

³W. A. Phillips, *Amorphous Solids: Low-Temperature Properties* (Springer-Verlag, Berlin, 1981).

⁴V. G. Karpov, M. I. Klinger, and F. N. Ignatev, *Sov. Phys. JETP* **57**, 439 (1983).

⁵T. S. Grigera, V. M. Mayor, G. Parisi, and P. Verrocchio, *Nature (London)* **422**, 289 (2003).

⁶A. P. Sokolov, R. Calemczuk, B. Salce, A. Kisliuk, D. Quitmann, and E. Duval, *Phys. Rev. Lett.* **78**, 2405 (1997); V. N. Novikov and A. P. Sokolov, *Nature (London)* **431**, 961 (2004).

⁷R. Bohmer and C. A. Angell, *Phys. Rev. B* **45**, 10091 (1992).

⁸M. B. Tang, H. Y. Bai, and W. H. Wang, *Phys. Rev. B* **72**, 012202 (2005); Yong Li, Peng Yu, and H. Y. Bai, *Appl. Phys. Lett.* **86**, 231909 (2005).

⁹J.-B. Suck, H. Rudin, H.-J. Guntherodt, H. Beck, J. Daubert, and W. Glaser, *J. Phys. C* **13**, L167 (1980).

¹⁰W. H. Wang, C. Dong, and C. H. Shek, *Mater. Sci. Eng., R.* **44**, 45 (2004).

¹¹R. Busch, E. Bakke, and W. L. Johnson, *Acta Mater.* **46**, 4725 (1998); D. N. Perera, *J. Phys.: Condens. Matter* **11**, 3807 (1999).

¹²K. Samwer and H. V. Lohneysen, *Phys. Rev. B* **26**, 107 (1982).

¹³T. Scopigno, G. Ruocco, F. Sette, and G. Monaco, *Science* **302**, 849 (2003).

¹⁴D. Huang and G. B. McKenna, *J. Chem. Phys.* **114**, 5621 (2001).

¹⁵M. A. Ramos, C. Talon, R. J. Jimenez-Rioboo, and S. Vieira, *J. Phys.: Condens. Matter* **15**, S1007 (2003).

¹⁶Because the excess entropy of SiO_2 at T_g is puzzlingly small and the thermodynamic m is related to the changes of the density of states in the vicinity of the BP [L. M. Martinez and C. A. Angell, *Nature (London)* **410**, 663 (2001) and references therein], the kinetic m of SiO_2 is not connected to its thermodynamic m , and then induces the anomaly in this correlation.

¹⁷V. Keppens, D. Mandrus, B. C. Sales, B. C. Chakoumakos, P. Dai, R. Coldea, M. B. Maple, D. A. Gajewski, E. J. Freeman, and S. Bennington, *Nature (London)* **395**, 876 (1998); R. P. Hermann, Rongying Jin, W. Schweika, F. Grandjean, D. Mandrus, B. C. Sales, and G. J. Long, *Phys. Rev. Lett.* **90**, 135505 (2003).

¹⁸A. Meyer, J. Wuttke, W. Petry, A. Peker, R. Bormann, G. Coddens, L. Kranich, O. G. Randl, and H. Schober, *Phys. Rev. B* **53**, 12107 (1996).

¹⁹P. H. Gaskell, *Nature (London)* **276**, 484 (1978).

²⁰S. Steeb and P. Lamparter, *J. Non-Cryst. Solids* **24**, 156 (1993).

²¹D. B. Miracle, *Nat. Mater.* **3**, 697 (2004).

²²H. Y. Bai, J. L. Luo, D. Jin, and J. R. Sun, *J. Appl. Phys.* **79**, 361 (1996).

²³W. Götze and L. Sjögren, *Rep. Prog. Phys.* **55**, 241 (1992).

²⁴H. Teichler, *Phys. Rev. Lett.* **76**, 62 (1996).

²⁵C. A. Angell, Yuanzheng Yue, Li-Min Wang, J. R. D. Copley, S. Borick, and S. Mossa, *J. Phys.: Condens. Matter* **15**, S1051 (2003).